Measurements in Polyphase Flows - 1982

Measurements in Polyphase Flows - 1982

presented at

1982 AIAA/ASME JOINT FLUIDS,
PLASMA, THERMOPHYSICS AND
HEAT TRANSFER CONFERENCE
ST. LOUIS, MISSOURI
JUNE 7-11, 1982

sponsored by

THE FLUIDS ENGINEERING DIVISION, ASME

edited by

T. R. HEIDRICK
ALBERTA RESEARCH COUNCIL
EDMONTON, ALBERTA

B. R. PATEL
CREARE INC.
HANOVER, NEW HAMPSHIRE

THE AMERICAN SOCIETY OF MECHANICAL ENGINEERS
United Engineering Center 345 East 47th Street New York, N. Y. 10017

Library of Congress Catalog Card Number 78-68328

FOREWORD

Accurate measurements of the fundamental physical variables of polyphase flows are an essential part of the development of many new process systems. Much of this development has stemed from the need to develop new energy systems—such as nuclear reactors, heavy oil production facilities and fluidized bed combustors, to name only a few. Measurements are required both in the field and in laboratory studies being done to validate models used to predict system performance. The symposia papers collected herein represent a compilation of current work being done to develop appropriate measurement techniques.

The papers generally describe:

. New measurement techniques or concepts in instrumentation.

. Results of experiments done to establish the accuracy and/or precision of measurement techniques or instruments.

. New methods or analytical models used to interpret the response of instruments in terms of the physical flow variables.

Measurements in various combinations of gas/liquid/solid flows are described.

The papers are divided into three sections:

I. Phase Distribution, Void Fraction and Density Measurements

II. Flow Rate and Axial Velocity Measurements

III. General Topics in Multi-Phase Flow Measurement

The first section consists of six papers primarily describing flow regime characterization or the measurement of some type of spatially averaged density or void fraction. The last paper describes how computerized tomographic reconstruction techniques may be used to convert spatially averaged measurements to local values.

The six papers contained in the second section describe measurement techniques for both globally averaged flow rates as well as local velocity measurements. A variety of techniques useful in the laboratory and in larger process application are presented.

The third section illustrates the diversity of problems encountered in polyphase flow measurement as a wide variety of problems and possible solutions are discussed.

We wish to thank all the authors and reviewers for their considerable efforts in contributing to this volume. We hope it will be useful to engineers and scientists engaged in multi-phase flow measurement development and application.

T. R. Heidrick

B. R. Patel

CONTENTS

A COMPARISON OF A RADIO FREQUENCY DENSITOMETER, CONDUCTANCE VOID GAUGE AND AN AUBURN 1080 MONITOR IN TWO-PHASE FLOWS

J. R. Nickerson
Atomic Energy of Canada Limited
Chalk River, Ontario, Canada

J. Whelpton and K. Smith
Canadian Astronautics Limited
Ottawa, Ontario, Canada

J. A. McKenna, Student
Department of Physics
University of Waterloo
Waterloo, Ontario, Canada

ABSTRACT

Cross-sectional average void fractions were measured in air/water, two-phase flows in a 38.1 mm ID horizontal tube using a radio frequency densitometer, a micro processor based conductance void gauge (CAL monitor), Auburn International Model 1080 Monitor and quick closing valves. The void fraction was varied over a 0-100% range with an average liquid mass flux of 1660 $kg \cdot m^{-2} \cdot s^{-1}$ and system pressure of 250 kPa. The radio frequency densitometer used was an E_{010} mode resonant cavity whose resonant frequency (577-661 MHz) depends on the average dielectric permitivity of the medium in the cavity. The CAL monitor uses a micro processor based system (Intel 8080A) which samples six conductance plates (and the fifteen possible combinations of conductance paths) in the instrument walls. The unit produced void fraction readings on a CRT, based on any desired time base and would display a PDF on an oscilloscope. The Auburn International Model 1080 uses a similar six-plate configuration but uses a rotating electric field and resistive summing networks to determine void fraction. The Auburn Model 1080 was the most linear of the devices but exhibited a parabolic shaped curve when compared with the quick closing valves. The radio frequency densitometer was fitted to the QCV corrected Auburn Monitor results with a third order polynomial with a standard deviation of fit of 4.2%. The radio frequency densitometer is recommended for any transient work due to its very high temporal resolution (10 msec).

INTRODUCTION

One of the fundamental quantities required to describe any two-phase flow is void fraction. The actual measurement may take several forms such as local, chordal average or cross-sectional average values. The type of void fraction measurement used and its success depends on the application [1,2]. Commonly applied local measurement methods include constant temperature anemometry, fibre optic probes, isokinetic sampling probe, conductance probes and microthermocouples. Chordal average methods usually employ γ, X-ray or neutron beam attenuation measurements. Cross-sectional average or volume average values may be measured by quick-closing valves, capacitance gauges, rotating electric field conductance gauges [3], neutron scattering techniques and presently with radio frequency resonant cavities.

In most industrial and transient measurements cross-sectional average values are normally sufficient and it is this mode of void fraction measurement that the present work is concerned with. Two types of void fraction measurement methods are studied, namely rotating field conductance and radio frequency (abbreviated RF) cavity devices. The three devices tested all offer moderately fast response (15-100 Hz), ease of operation and minimal flow perturbation such that they are called nondisruptive but nevertheless intrusive. The RF cavity is a newly designed void gauge which is a field device whose resonant frequency depends on the mixture dielectric permitivity. This type of device (RF cavity) has been used before for hydrogen density measurements [4], but we believe its application in this role to be unique.

DESIGN AND PRINCIPLE OF OPERATION

Auburn Monitor

The Auburn* 1080 Monitor used in this study was the first production model of this type and consists of three main components: main flow sensor, electronics unit and reference sensor. The main sensor consists of six 229 mm long, stainless steel electrodes separated by ceramic insulating strips forming a twelve-sided polygon with a dimension across the electrodes of 38.1 mm.

The plate configuration of the Auburn sensor forms three opposed electrode pairs which are excited with a 5 kHz, 10 V sinusoidal signal, with each electrode pair excited 120 deg. out of phase with the others. Across each electrode pair a conductance circuit measures the absolute conductance and the three individual conductances are summed in a resistor network with the resultant being proportional to the average mixture density. This sum is passed through an analog divider where it is divided by the conductance from the reference sensor and this output is displayed. The reference sensor must be placed in the single-phase liquid only line and is used to compensate for any variations in the liquid conductivity.

*Auburn International Inc., Danvers, Mass.

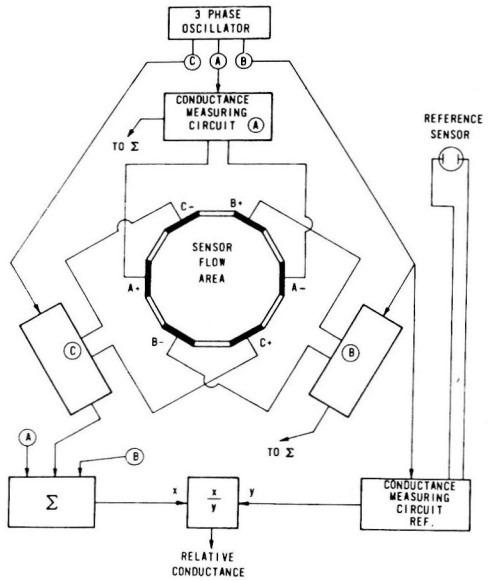

FIGURE 1 SCHEMATIC DIAGRAM OF THE CONDUCTANCE MONITOR

Reference 3 gives a full description of the device and illustrates the rotating electric field vector. Figure 1 is a schematic of this conductance monitor system and is reproduced from [3] with the permission of the senior author.

Cal Monitor

The conductance void gauge (named the CAL monitor) uses an identical reference and flow sensor arrangement except for material and minor geometry changes. The signal processing and electrode excitation technique, however, is done digitally. The CAL monitor uses a micro-processor based system (Intel 8080A) which samples the six conductance plates and the fifteen possible conductance paths*. The microprocessor controls analog switches which apply a voltage between any electrode pair. The conductivity is computed from the current via an A/D converter and then the polarity is reversed and the readings repeated and averaged to compensate for any electrochemical effects. The path conductivity is computed and corrected for the three different path lengths. Uncovered electrodes (as is the case for stratified flow) will give a near zero conductivity and these values are not used in computing void fraction. The resultant mixture conductivity from the data obtained from "live" electrodes is normalized by the value determined from a reference sensor. The output may be displayed digitally on a CRT or teletype through an RS232 interface or on a chart recorder or oscilloscope through a D/A converter. The unit has a sample and compute rate of about 25 Hz, a slightly higher response than that for the Auburn 1080. The CAL monitor has various modes of void fraction display and can integrate the void fraction over a period of time (user specified) or perform a probability density function (PDF) analysis on the signal and display the PDF on an oscilloscope. Another mode is to collect and average a specified number (up to 512) of void fraction results and store the results to be displayed later on an oscilloscope to form a time history.

RF Void Fraction Gauge**

In this technique the resonant frequency of an RF cavity depends on the dielectric permitivity of the mixture flowing through it and thus is a measure of void fraction. The dielectric permitivity ratio for air to water is about 30 to 1 for room temperature and atmospheric conditions decreasing to about 10 to 1 for high pressure (10 MPa) steam-water systems. The success of the technique depends on the liquid medium having a sufficient low loss tangent so that small powers may be used to excite the cavity.

*Patents covering rotating electric field devices such as this for conductance and capacitive measurement techniques for void fraction measurement are held by Auburn International Inc.

**Patents applied for by Atomic Energy of Canada Limited

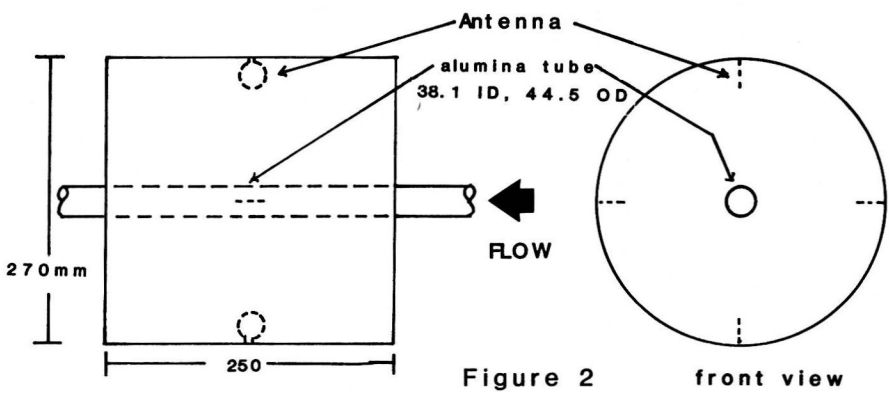

Figure 2 RF Void Gauge

For water the loss tangent is a minimum around 300 MHz at 95°C and decreases with increasing temperature and increases slowly with frequency up to 1 GHz. Thus an upper frequency limit (and consequently size scale) should be around 1 GHz and below. The diameter of cavity is set by the resonant frequency and the relative dielectric permitivity of the medium the cavity. The diameter of the cavity may be made smaller by a factor of approximately the square root of relative dielectric permitivity of the surrounding medium. For example, if a cavity were filled with aluminum oxide (relative dielectric permitivity of 8 or higher) it would be a factor of approximately 3 smaller in diameter than a free air cavity. For this study the RF instrument consisted of 27 cm diameter, 25 cm long aluminum cylinder forming the resonant cavity excited in the E_{010} mode by coupling loops, 90° apart in the mid-plane of the cylinder (see Figure 2). Along the centreline and passing through the cylinder end walls in an alumina tube (38.1 mm ID and 3.1 mm thick) through which the two-phase mixture flows. The coupling loops are 0.1 square wavelengths in area and the cavity is filled with a dielectric medium (aquarium gravel in this case) to reduce the resonant frequency of the cavity. A cylindrical cavity excited in the E_{010} mode has rotational symmetry of the E field about the longitudinal axis with a field maximum in centre and falling to zero at the walls. The E field is also fairly flat in the central region and consequently the device is not sensitive to the way in which the phases are distributed in the mixture. The four coupling loops or antennas for the device are placed 90° apart (to avoid direct coupling by excitation of the TE_{111} mode) and two are excited (with a sweep frequency generator†) 90° out of phase through a 90° hybrid. The other two antennas are coupled through a 90° hybrid and act as the receiving loops with the resultant signal fed into a crystal detector†† and then through a log amplifier and displayed on a CRT†††. The CRT displays an energy versus swept frequency characteristic for the cavity at any given time.

Calibration

All three devices were mounted in a small two-phase flow (air-water) loop where they could be calibrated with quick-closing valves.

The test section is a horizontal 4 m long section made of 38.1 mm ID lucite tubing. The main sensors were located between spring loaded quick-closing valves (QCV's) 1.37 m apart and 2 m downstream of an air-water mixer. The QCV's were coupled by steel rods to guarantee simultaneous closure in approximately 25 ms. Liquid trapped between the valves could be drained into a graduated cylinder to obtain the global void fraction of the section.

† Wiltron 610b and 640 G50
†† Wiltron 7N50 detector
†††Wiltron 640 system, 640E Log Amp.

The air and water flows were independently metered to give a 0-100% range of void fraction and 0-2.3 $m \cdot s^{-1}$ liquid superficial velocity (average mass flux of 1660 $kg \cdot m^{-2} \cdot s^{-1}$) and maximum air superficial velocity of 70 $m \cdot s^{-1}$. The average system pressure was 250 kPa with a maximum pressure of 540 kPa. After flow conditions were set and allowed to stabilize, the void fraction was noted after a ten second averaging time (set internally on the CAL monitor and with an integrating digital voltmeter with the Auburn monitor) and the QCV's were closed and the liquid remaining measured. The actual QCV void fraction was taken as the average of three QCV closures.

Results and Discussion

The comparison of the relative conductivity measurement by the Auburn monitor versus the QCV void fraction is shown in Figure 3. It may be noted that the curve is somewhat non-linear and does not have the same trend as given in [3] in the higher void ranges. A possible explanation for this was due to internal circuity changes made on the Auburn 1080 necessitated by component failures. Another factor could be the orientation of the sensor in that an insulator or conductance plate may be located at the bottom. (In these tests an insulating strip was oriented at the bottom of the sensor.) This would affect the void fraction readings in the annular flow regime due to eccentricity in the liquid film thickness on the sensor walls. Maxwell's expression [5] is given by:

$$1 - \frac{k_m}{k_o} = 3\alpha(2+\alpha)$$

k_m = mixture conductivity
k_o = liquid conductivity
α = void fraction

This expression, derived for non-interacting, equal sized spheres of zero conductivity distributed in a continuous medium, is also plotted on Figure 3.

The Bruggeman relation [6] is given by

$$1 - \frac{k_m}{k_o} = 1 - (1-\alpha)^{3/2}$$

α, k_m, k_o as before.

This expression considers the mixture to be composed of randomly sized spheres of zero conductivity and is plotted on Figure 3 along with a polynomial (coefficients given in Table 1) which fits the data to a standard deviation of 3.7%.

The Maxwell and Bruggeman expressions show remarkable agreement with the data, however, there is no theoretical basis for extending them beyond 30% void fraction where the transition from bubbly flow generally took place in this experiment.

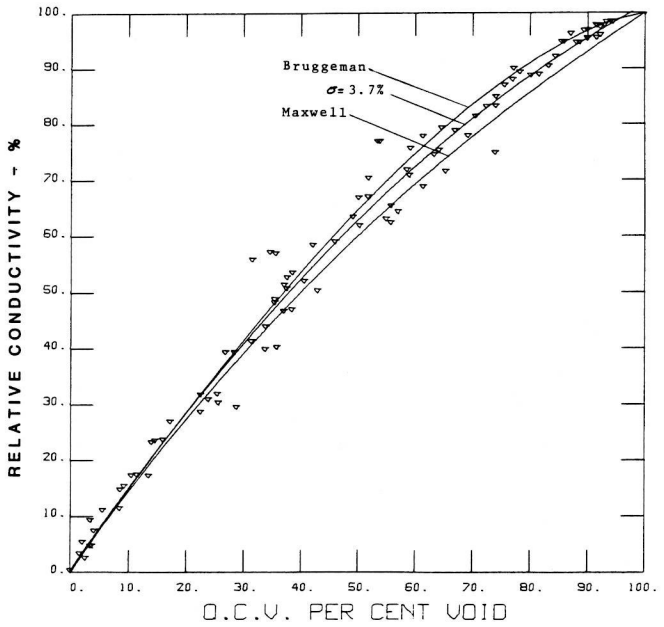

FIGURE 3

Figure 4 shows the relative conductivity (void fraction) measured by the CAL monitor plotted against the QCV void fraction. The high non-linearity is attributed to the way in which the three different conductivity paths are weighted to get the mixture conductivity. The weighting constants were based on liquid only measurements and this is not representative of the conduction paths in a two-phase mixture. The line plotted on Figure 4 is a cubic equation given in Table 1 which fits the data with a standard of deviation of fit of 8.5%.

Since the resonant frequency of the RF cavity depends on the mixture dielectric permitivity it was decided to plot a non-dimensional frequency ratio versus void fraction. The non-dimensional frequency ratio was taken as:

$$\text{Frequency ratio} = \frac{f_w - f_m}{f_w - f_o} \times 100\%$$

f_m = resonant frequency for the mixture
f_o = resonant frequency for air = 577 MHz
f_w = resonant frequency for water = 661 MHz

This was plotted against the corrected Auburn monitor relative conductivity (or termed correlated QCV void) in Figure 5. Because of mechanical interference between the RF cavity and the control rods for the QCV's the RF cavity was compared with the corrected Auburn data as the QCV's had to be incapacitated to perform this part of the test.

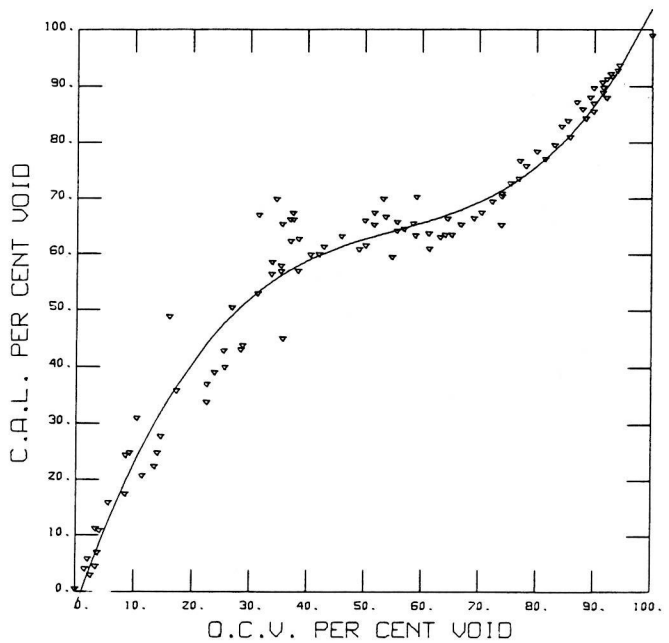

FIGURE 4

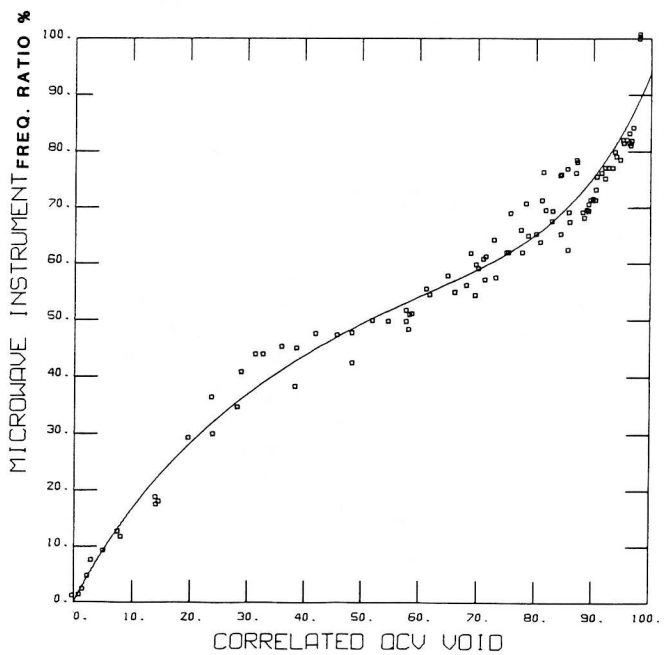

FIGURE 5

The "S" shaped curve is due to a non-linear transfer function between the frequency ratio and void fraction (see Table 1). The slight degree of scatter in the data was due to difficulties in reading the resonant frequency of the cavity. The scope display for this experiment had an energy versus frequency display with a graduated frequency scale. The resonant peak was observed to shift rapidly and average frequencies were estimated by eye.

The conductivity devices used measure the relative conductivity of the mixture or in essence some measure of the liquid film thickness between electrodes. In annular flow it is expected that the accuracy will be limited by the degree of entrainment of liquid drops to which there is no conductance path. This limitation has been recognized [3], however, over the range of mass fluxes encountered it did not represent a significant error. The RF cavity method of determining void fraction does not suffer from this limitation since it is a field technique. All the methods tested are fairly simple techniques, easy to apply and generally non-disruptive (but intrusive) for void fraction measurement. The RF cavity has a very high response rate, 10 ms for an instantaneous reading, limited by sweep rates and video detectors. A simpler method of measuring the resonant frequency of the cavity by the use of ordinary frequency counters could be realized through using a resonant frequency tracking system or cavity tuned oscillator [4]. This possibility is being examined and modifications to CAL monitor are planned to improve its linearity and to try to compute rough void distributions and to identify flow regimes.

ACKNOWLEDGMENTS

The authors wish to extend their thanks to S.M. Carr for his assistance on the calibration section of the experiments and to J.H. Woodall and T.A. Kennedy for their assistance on the QCV's.

REFERENCES

1. Hewitt, G.F., "The Role of Experiments in Two-Phase Systems with Particular Reference to Measurement Techniques," Progress in Heat and Mass Transfer, Vol. 6, 1972.
2. Jones, O.C., Delhaye, J.M., "Transient and Statistical Measurement Techniques for Two-Phase Flows: A Critical Review," Int. J. Multiphase Flow, Vol. 3, No. 1, July 1976.
3. Merilo, M., Dechene, R.L., Cichowlas, W.M., "Void Fraction Measurement with a Rotating Electric Field Conductance Gauge," J. of Heat Transfer, Vol. 99, No. 2, May 1977.
4. Wenger, N.C., Smetana, J., "Hydrogen Density Measurements Using an Open-Ended Microwave Cacity," IEEE Trans. on Inst. and Meas., Vol. IM-21, No. 2, May 1972.
5. Maxwell, J.C., "A Treatise on Electricity and Magnetism," Clarendon Press, Oxford, 1881.
6. Bruggeman, D.A.G., "Berechnung Verschiedener Physikalischer Konstanten von Heterognem Substanzen," Ann. Phys., Leipzig, Vol. 24, 1935, p. 636.

TABLE 1

Device R=Device Reading in %	$\alpha = a + bR + CR^2 + dR^3$				
	a	b	c	d	σ
CAL	4.40439	-0.26562	0.02143	-0.00008	8.5%
Auburn	-1.38736	0.89126	-0.00492	0.00006	3.7%
RF	-2.66467	1.77273	-0.10888	0.00370	4.2%

FLOW REGIME CHARACTERIZATION AND LIQUID FILM THICKNESS MEASUREMENT IN HORIZONTAL GAS-LIQUID TWO-PHASE FLOW BY AN ULTRASONIC METHOD

J. S. Chang
Department of Engineering Physics and Institute for Energy Studies
McMaster University
Hamilton, Ontario, Canada

Y. Ichikawa and G. A. Irons
Department of Metallurgy and Materials Science
McMaster University
Hamilton, Ontario, Canada

ABSTRACT

A technique, using an ultrasonic, has been developed to measure liquid film thicknesses and to characterize flow regimes in horizontal gas-liquid and gas-liquid metal two-phase flows. The effect of tube size, tube wall thickness and liquid film temperature are discussed.

I. INTRODUCTION

A technique, using ultrasonics, has been developed to measure liquid film thicknesses and to characterize flow regimes in gas-liquid and gas-liquid metal two-phase flows. The technique is potentially applicable to flow in high-pressure metallic pipes or high temperature liquid-metal systems where other techniques based on capacitance, optical or conductance principles cannot be used. The technique is also practical in large volume pipes or vessels and for measurement of fast-transient phenomena (up to order of μsec), in which case, radiation techniques are restricted to thin pipes and require a strong source and a large amount of radiation shielding to observe fast, transient phenomena. There are three ultrasonic methods which exist for two-phase flow diagnostics, namely the pulse echo, the transmission and the Doppler shift methods.

One of the most widely used ultrasonic techniques in the single phase fluid dynamics is based on the Doppler effect. Lahey [1] modified this type of method in two-phase flow. However, the results indicated that single bubble velocity could be measured, but data integration becomes difficult when many bubbles are present. Chang et al [2] used the transmission method to measure void fraction in the bubbly flow. They observed that the method is very useful for measurement of relatively small void fraction ($0 < \varepsilon_g \leq 20\%$) with the accuracy of $\pm$ 1%. Pulse Echo methods was used by Lahey [1] and Chang et al [2] to observe the location and size of the single bubble. The principle used for present thickness measurement is based also on the pulse-echo technique which is similar to sonar. A sound pulse is sent through the gas-liquid or wall-liquid interface and travels back. The transit time of the pulse gives a measure of the distance between interface (e.g. bubbly flow, flow through an annulus); however, a detailed waveform analysis is required.

In this paper, flow regime characterization by a double ultrasonic transducer method has been developed in addition to liquid film thickness measurement techniques using a single ultrasonic transducer. The effect of temperature gradients inside films and the effect of tube size and wall thickness are also discussed.

2. PRINCIPLE OF ULTRASONIC DIAGNOSTICS

(i) Principle of Ultrasonic Liquid Thickness Measurement

In stratified gas-liquid flow through a cylindrical pipe such as shown in Figure 1a, one part of sound pulse discharged from the transducer will be reflected by a tube wall-liquid interface, and received by the same transducer. The remainder of the pulse will be transmitted through the liquid and then reflected back to the transducer from liquid-gas interfaces. Therefore, if we plot the various signals received over a period of time from the transducer as an oscilloscope would see them, we obtain waveforms as shown in Figure 1b. It should be noted that attenuation during transmission through condensed phases (solids and liquids) and at interfaces between them is small compared to that in a gas, for ultrasonics in the MHz range. This is due to the fact that the acoustic impedence of a gas is much smaller than that of liquids or solids. The transit time of a pulse, Δt can be converted to the distance between the interfaces, if the sound velocity is known. This same principle also applies when there is more than one interface, for example annular tubes.

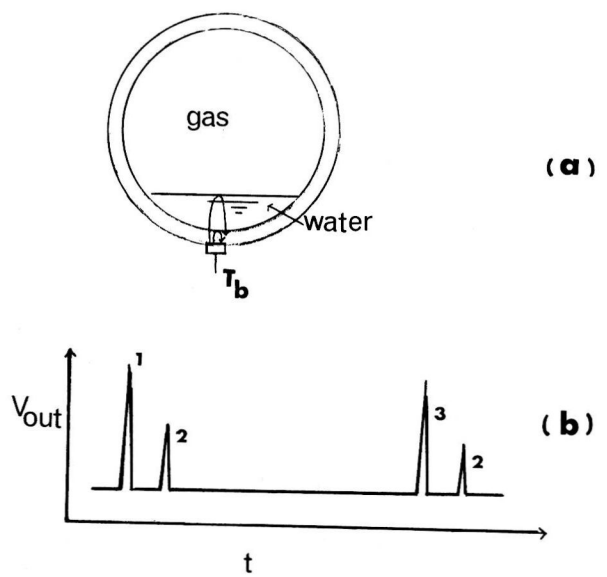

Fig. 1: Schematic of stratified gas-liquid flow through a cylindrical pipe and ideal ultrasonic waveform.

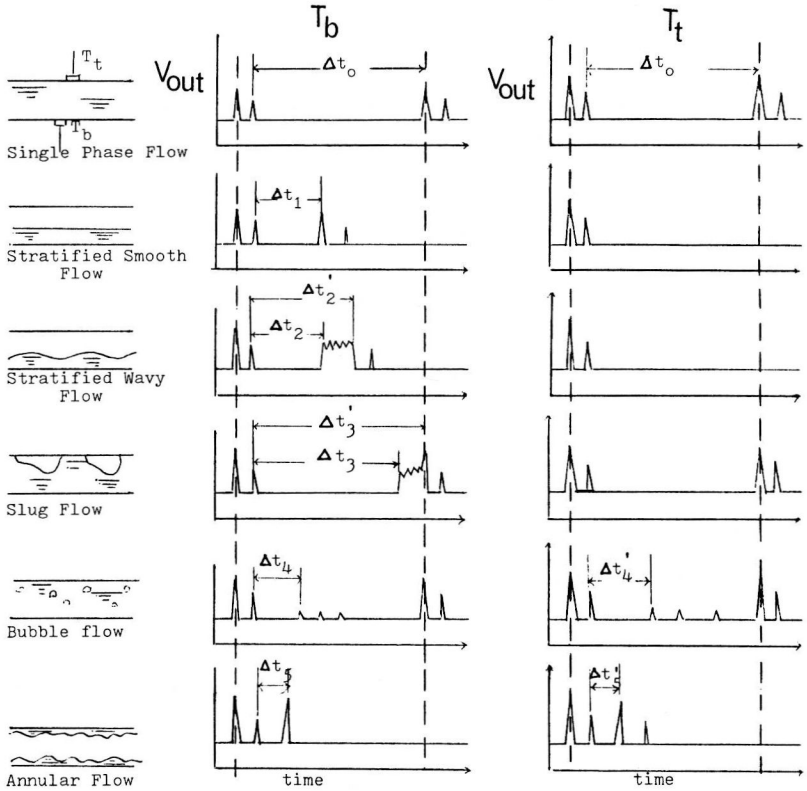

Fig. 2: Schematic of flow patterns in horizontal two-phase flow and its ideal ultrasonic waveforms;
T_b: waveforms from transducers at top of tubes;
T_t: waveforms from transducers at bottom of tubes.

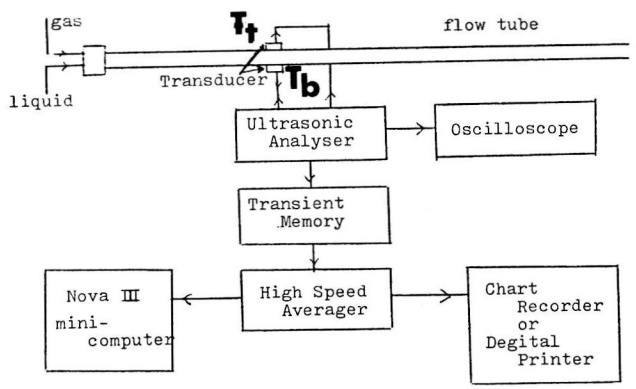

Fig. 3: Schematic of flow and ultrasonic film thickness measurement system.

There are two other considerations that arise from the fundamental physics of ultrasonics [3]. If the liquid phase is moving with velocity U_f, a correction due to the Doppler shift is necessary if U_f approaches sound speed a. In addition, the thickness measurement is restricted by the ultrasonic frequency. If the frequency of sound wave is f, the minimum thickness that can be measured is approximately $d_{min} \simeq a/f$.

(ii) Principles of Ultrasonic Flow Regime Characterization in a Horizontal Two-Phase Flow

During horizontal, cocurrent gas-liquid flow in pipes, a number of flow patterns, normally called regimes, are found to exist. These result from the particular manner in which the gas-fluid flow is distributed in the pipe. Even though most authors define flow regimes somewhat differently, most agree on six different flow regimes. These are shown in Figure 3.

The following definitions will be the ones used in this paper. Stratified smooth flow occurs when the fluid is at the bottom of the pipe and the gas flows along the top. The surface of the fluid is smooth. Stratified wavy flow is similar to stratified smooth; however, the gas-fluid interface is wavy instead of smooth. Both elongated bubble (this is also designated as plug flow) and slug flow, and what Taitel and Dukler [5] call intermittent flow are characterized by the fluid bridging gap between gas-fluid interface and the top of the pipe. The difference between slug and plug flow depends on the degree of agitation of the bridge. This work follows the definition of Taitel et al [6]. Plug flow is considered to be the limiting case of slug flow where no entrained bubbles exist in the fluid slug.

Annular flow occurs when the walls are wetted by a thin film of fluid while gas at high velocity flows through the centre of the pipe. Fluid droplets are usually entrained in this gas. When the upper walls are intermittently wetted by large aerated waves sweeping through the pipe, it is not slug flow, which requires a complete fluid bridge, nor annular flow which requires a stable film. Again following Taitel

et al [6], this has been designated as wavy annular flow. This regime was not recognized by Mandhane et al [4] and was considered to be slug flow.

The last regime is the dispersed bubble or bubbly regime. The fluid completely fills the pipe while small gas bubbles are distributed throughout the body of the pipe. The transition to this regime is characterized by the gas bubbles losing contact with the top of the pipe. At first, the bubbles are near the top of the pipe, but become more uniformly distributed at higher liquid flow rates.

Using the fundamental principles of ultrasonics in Section 2(i), we can extend the technique to the more complicated regimes described above. Let us now consider two transducers, one on the top T_t and the other on the bottom T_b of a horizontal pipe which produces the pulse. The anticipated output integrated over a period of time for the various regimes would appear as pictured schematically in Figure 2.

For a single phase flow, tube full with liquid, output signals for T_b and T_t are identical, and we can determine sound velocity from Δt. For a stratified smooth flow, we can determine liquid level from Δt, of T_b. We also can determine the amplitude of the surface wave as well as liquid level from Δt_2 and Δt_2 of T_b in the case of stratified wavy flow. In the stratified flow case, we only observed tube wall-gas interface in T_t output since no pulse is transmitted through the gas phase. For slug flow, the T_b output is similar to stratified wavy flow, except that signals corresponding to slug attached to the top wall will be shifted in time, and furthermore, the T_t output is much different from wavy flow. From the $\Delta t_4''$ and $\Delta t_4'$ in T_b and T_t outputs, respectively, we also may identify the bubbly flow as well as average location of bubbles. The signal output of annular flow is similar to stratified flow; however, the signals corresponding to gas-liquid interface will appear in both T_b and T_t outputs.

3. EXPERIMENTAL APPARATUS

A schematic of the single pulse ultrasonic liquid film thickness measurement system is shown in Figure 3. The ultrasonic pulse is generated by a Panametrics 50524UA ultrasonic analyzer, and discharged from a contact probe transducer. A Panametrics 2.25 MHz 6mm diameter A533S transducer was used in the present study. The reflected wave was received by the same transducer and handled by the ultrasonic analyzer. The output signal could be displayed on a TEKTRONIX 468 digital storage oscilloscope or stored in a Kawasaki MR-50E transient memory equipped with a Kawasaki TMC-300 high speed averager. For more detailed analysis of the waveforms, the output of the transient memory or averager could be dumped into a NOVA III minicomputer or an individual output could be displayed in a conventional chart recorder or digital printer. The cocurrent air-water two-phase flow was generated by a 1.9 cm I.D. 180cm long, 3.2mm thick lucite pipe in the horizontal position as shown in Figure 3. Air and water is taken from the laboratory supply at approximately room temperature and atmospheric pressure. It passed through filters and then entered the mixing section through a pressure regulator and rotameter. The measurement section was located 150cm from the mixing section; therefore, the flow was fully developed. The air-mercury two-phase flow was generated by a 2.4 cm. I.D. 48cm long, 6.4mm thick lucite pipe, in which only the air was flowing. Horizontal cylindrical tubes with 19.1, 25.4, 38.1 and 50.8mm I.D. were also used to examine reflected wave forms for film thickness measurements.

4. EXPERIMENTAL RESULTS

(i) Film Thickness Measurement

Typical ultrasonic waveforms, corresponding to air-water stratified flow through 5.08cm I.D., 6.4mm thick horizontal single tubes are shown in Figure 4, where the numbers 1, 2 and 3 in the figures are corresponding to the initial, wall-liquid and liquid-gas pulses, respectively. Figure 4 shows that the attenuation of ultrasound is not very great in lucite and water; therefore, we may determine liquid film thickness not only from the first set of reflected signals, but also from the second or third set of reflected signals. Similar typical ultrasonic wave-

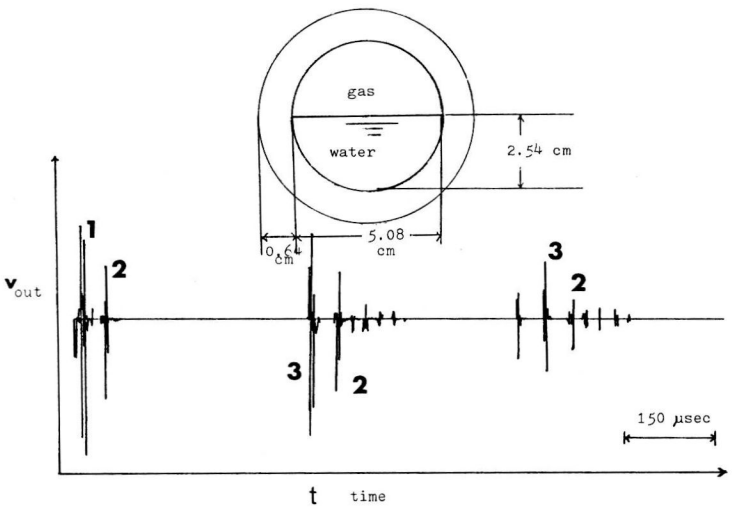

Fig. 4: Typical ultrasonic waveforms corresponding to air-water stratified flow through 5.08 cm I.D., 6.4 mm thick horizontal single tubes. 1. initial signal; 2 wall-liquid interface; 3. liquid-gas interface.

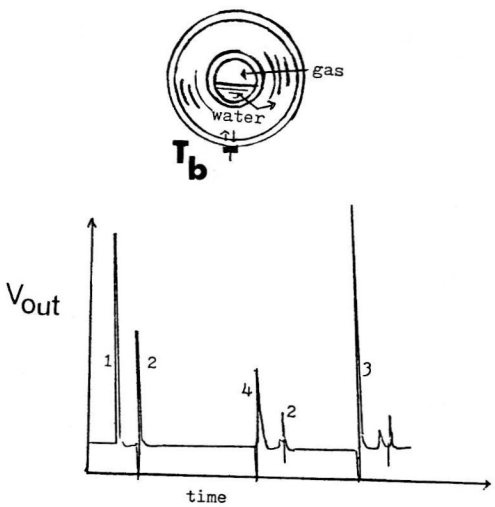

Fig. 5. Typical ultrasonic waveforms corresponding to air-water stratified system in the horizontal annular tubes. 1. initial signal; 2. wall-liquid interface; 3. liquid-gas interface; 4. liquid-wall interface.

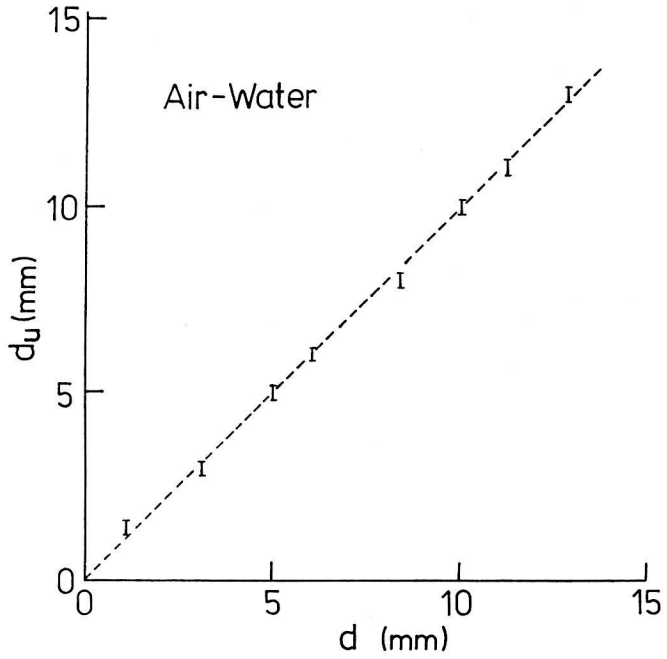

Fig. 6
Comparisons between liquid film thickness measurements by an ultrasonic method. d_u, and calculated liquid film thickness, d, in a horizontal air-water stratified system.

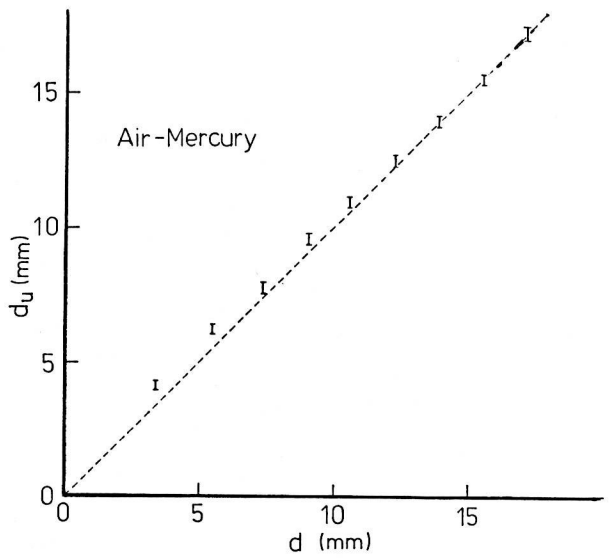

Fig. 7
Comparisons between liquid film thickness measurements by an ultrasonic method and calculated liquid film thickness in a horizontal air-mercury stratified system.

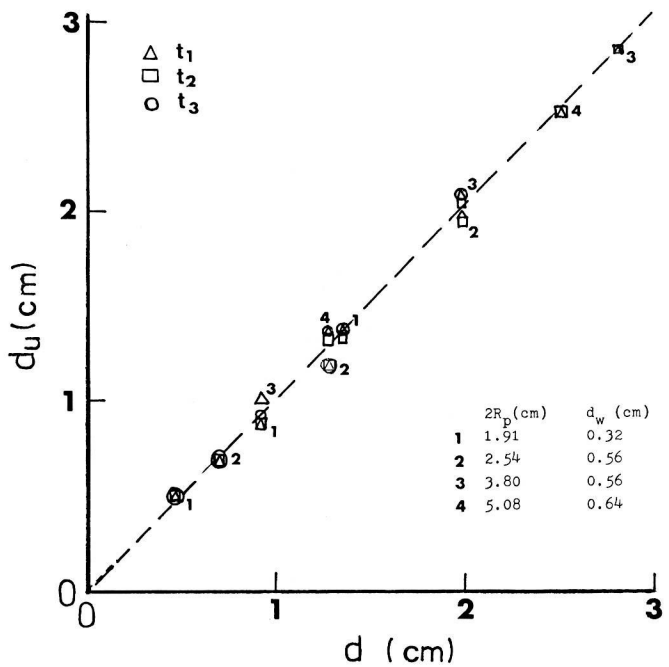

Fig. 8
Effect of tube size, and wall thickness and using 2nd set of reflection on the ultrasonic thickness measurements.

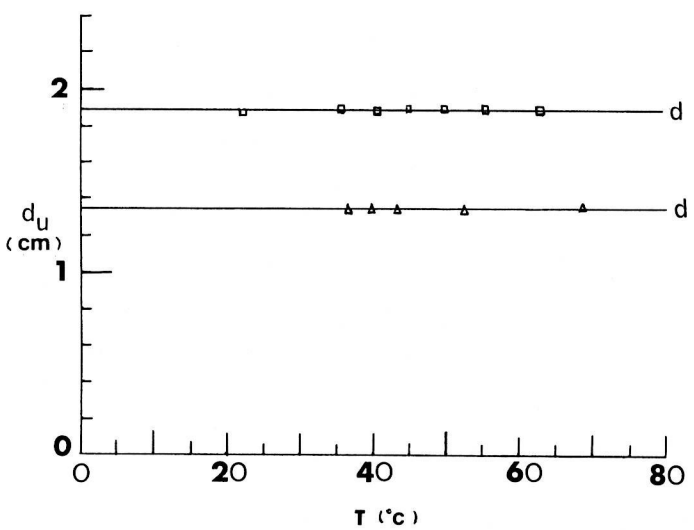

Fig. 9
Effect of liquid temperature and temperature gradient in an ultrasonic liquid film thickness measurement.

forms corresponding to air-water stratified system in the horizontal annular tube is shown in Figure 5, where the numbers in Figure 5 correpond to the same definitions as in Figure 4, except 4 is liquid-wall interface in this figure. From Δt in Figures 4 and 5, we can determine liquid film thickness in both single and annular tubes.

The results of liquid film thickness measurements in stratified air-water and air-mercury systems in the 2.54cm I.D., 6.4mm thick lucite tube are shown in Figures 6 and 7, respectively, where d_u and d in the figure correspondent to the liquid film thickness measured from ultrasonic waveform and calculated value from known amount of water introduced into the cylindrical container respectively. One can observe that there is good agreement between d_u and d, except for a small discrepancy in the air-mercury system. This error is due to the relatively large effect of the meniscus for small volumes of mercury when calculating the expected thickness d simply from the volume placed in the cylinder.

The results of the liquid film thickness measurements in stratified air-water systems using first, second and third sets of reflected signals in various sizes of horizontal cylindrical containers are shown in Figure 8. Figure 8 shows that the results using first, second or third sets or reflected signals agree well with each other for every different size of tubes.

The effect of water temperature gradient inside the film on the film thickness measurement is shown in Figure 9, where 3.8cm I.D., 5.6mm thick horizontal cylindrical tube is used in this study with surface and bottom water temperature ranges from 20°-78°C and 20°-76°C, respectively. The temperature was determined by a radially moveable micro thermocouple, and temperature dependence of sound velocity was determined from standard tables [Rivkin et al, 7]. The effect of a temperature gradient was negligible as Figure 9 indicates.

(ii) Flow Regime Characterization

Typical ultrasonic waveforms received by T_b transducer for various flow regimes in a horizontal cocurrent air-water two-phase flow are shown in Figure 10. In this case, the output waveforms are single pulse signals averaged over a period between a few milliseconds and a second. Figure 10 shows that very clear flow regime characterization can be achieved with the present techniques discussed in Section 2. Similar typical ultrasonic waveforms received by T_b transducer for various flow regimes in horizontal cocurrent air-mercury two-phase flow are shown in Figure 11. Figure 11 shows that flow regime can be characterized in air-mercury. Here the flow regimes in Figures 10 and 11 were also determined from visual observations and thus, only clearly differentiated cases are presented in Figures 10 and 11.

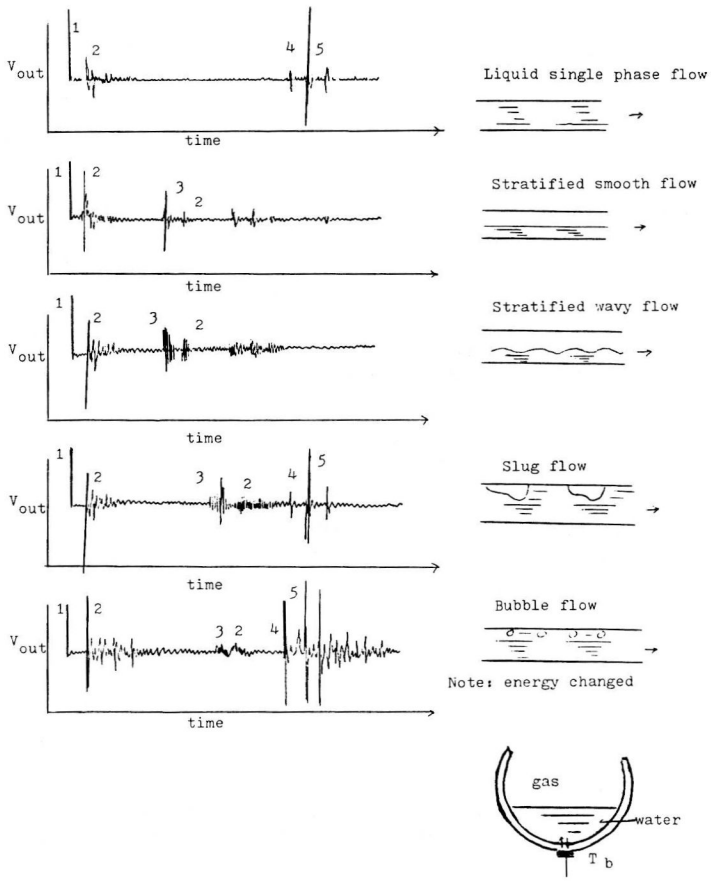

Fig. 10: Typical time averaged ultrasonic waveform for various flow regimes in a horizontal air-water two-phase flow. 1. initial signal; 2. wall-liquid interface; 3. liquid-gas interface; 4. liquid-wall interface; 5. wall-gas interface.

5. CONCLUSIONS

A technique, using an ultrasonic, has been developed to measure liquid film thickness and to characterize flow regimes in a horizontal gas-liquid and gas-liquid metal two-phase flows, and the following conclusions have been obtained:

(1) the liquid film thickness measured ultrasonically agrees with real film thickness for fluids in which the sound velocity of fluid was known.
(2) the effects of liquid film temperature and temperature gradient in film were observed to be minor.
(3) very clear flow regime characterization can be achieved with the present ultrasonic method.

ACKNOWLEDGEMENTS

The authors wish to express their appreciation to Drs. W-K. Lu, J. Chan, V.S. Krishnan, S. Banerjee and M. Doby for valuable discussion and comments. They also wish to express their gratitude to E. Morala and J. Fidley for the technical assistance. This work was supported by the National Science and Engineering Council of Canada.

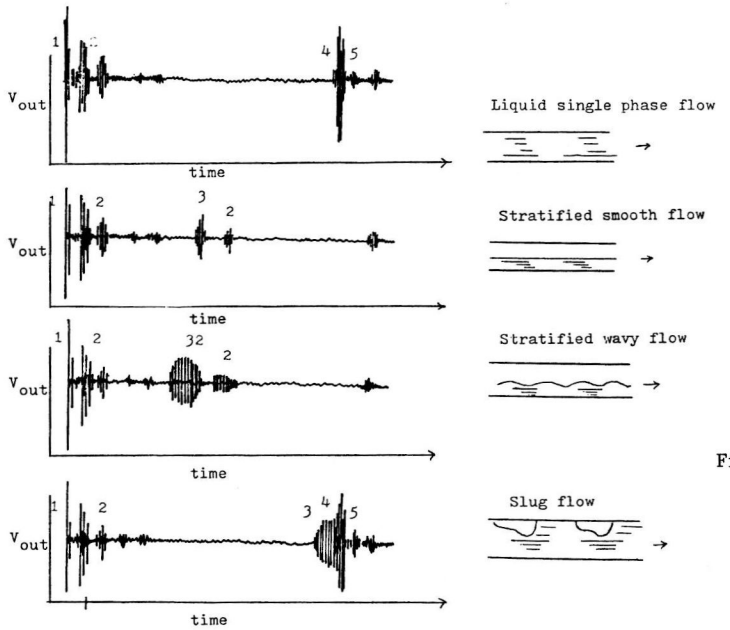

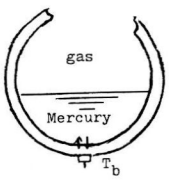

Fig. 11: Typical time averaged ultrasonic waveform for various flow regimes in a horizontal air-mercury two-phase flow. 1. initial signal; 2. wall-liquid interface; 3. liquid-gas interface; 4. liquid-wall interface; 5. wall-gas interface.

REFERENCES

1. R.T. Lahey, "A Review of Selected Void Fraction and Phase Velocity Measurement Technique", Lecture presentation at Fluid Dynamics Institute Short Course on Two Phase Flow Measurements, Darmouth College, 1978. In. Adv. Nucl. Sci. & Tech., vol. 13, pp. 396-398 and pp. 297-298, by S. Banerjee and R.T. Lahey, 1981.

2. Jen-Shih Chang, Y. Ichikawa, G.A. Irons and E. Morala, "Developments of Ultrasonic Void Fraction Diagnostic Technique for Bubbly Flows", In Annual Report of the Thermal Hydraulics and EHD Research Laboratory, McMaster University, 1981.

3. J. Krauthramer and H. Krauthramer, "Ultrasonic Testing of Materials", Springer-Verlag, New York, 1969.

4. J.M. Mandhane, G.A. Gregory and K. Aziz, "A Flow Pattern Map for Gas Liquid Flow in Horizontal Pipes", Intern. J. Multiphase Flow, vol. 1, 1974, pp. 537-553.

5. Y. Taitel and A.E. Dukler, "A Model for Prediction Flow Regime Transitions in Horizontal and Near-Horizontal Gas-Liquid Flow", A.I.Ch.E. J., vol. 22, 1976, pp. 47-54.

6. Y. Taitel, B. Barmen and O. Shoham, "Flow Pattern Transition for Gas-Liquid Flow in Horizontal and Inclined Pipes", Intern. J. Multiphase Flow, vol. 6, 1979, pp. 217-225.

7. S.L. Rivkin, A.A. Aleksandrove and E.A. Kremenvskaya, "Thermodynamics Derivations for Water and Steam", John Wiley & Son, 1978.